Design and Modeling of a Textile Pressure Sensor for Sitting Posture Classification

Jan Meyer, Bert Arnrich, Johannes Schumm, and Gerhard Tröster, *Senior Member, IEEE*

***Abstract*—A textile pressure sensor has been designed for measuring pressure distribution on the human body. Electrodes built with conductive textiles are arranged on both sides of a compressible spacer, forming a variable capacitor. The use of textiles makes unobtrusive, comfortable, lightweight, and washable sensors possible. This simplifies the goal to integrate such sensors into clothing in the future, to be simple, and fast to mount just as getting dressed.**

Hysteresis induced by the spacer of the sensor has been modeled with the Preisach model to reduce the measurement error from 24% to 5% on average and the maximal error from above 50% to below 10%. Standard textiles that are not specially optimized for low hysteresis can be used for designing the sensor due to the modeling. The model may also be used for other pressure or even strain sensors to reduce their hysteresis. The modeling enhances the accuracy of the textile sensor to those of commercial, nontextile pressure sensing mats.

Furthermore, we used the sensor system for the classification of sitting postures in a chair. The data of nine subjects have been classified with Naïve Bayes classifier, achieving an average recognition rate of 82%. We show that the textile sensor performs similarly to a commercial, nontextile pressure sensing mat for this application.

***Index Terms*—Hysteresis modeling, posture classification, textile pressure sensor.**

I. Introduction

BODY-worn sensors serve as input devices for many applications in wearable computing, such as in the area of sports, personal health care [1], or guidance of workers [2]–[4] and fire fighters [5].

Integrating such sensors directly into clothing has several advantages. Clothing is worn almost anytime and is an ideal substrate for mounting sensors with direct contact to the body. They are just at the right place on the body once dressed, and the user does not need to care about positioning them. Textile solutions are favorable to obtain a sensing system that is comfortable and unobtrusive to the wearer. When textile elements are used for constructing the sensors, future integration into clothing is simplified compared to mount discrete electronic sensors; also, washability can be better achieved with textiles. Textiles have been used for pressure [6], stretch [7], and temperature [8], [9] sensing.

Manuscript received January 07, 2009; revised September 23, 2009; accepted November 06, 2009. Date of current version May 26, 2010. The associate editor coordinating the review of this paper and approving it for publication was Dr. Patrick Ruther.

The authors are with the Wearable Computing Laboratory, Department of Information Technology and Electrical Engineering, Swiss Federal Institute of Technology Zurich, CH-8092 Zurich, Switzerland (e-mail: meyer@ife.ee.ethz.ch; barnrich@ife.ee.ethz.ch; schumm@ife.ee.ethz.ch; troester@ife.ee.ethz.ch).

Color versions of one or more of the figures in this paper are available online at http://ieeexplore.ieee.org.

Digital Object Identifier 10.1109/JSEN.2009.2037330

However, textiles are usually not optimized for sensing purposes, e.g., hysteresis provoked by compressed or stretched material influences the measurement of pressure or stretch sensors. Such influence can be reduced by modeling the textile behavior to compensate the errors induced. The modeling enhances the flexibility in material selection for the sensor; it is not necessary to use material that is optimized for low hysteresis.

In this paper, we present a capacitive textile pressure sensor. The design of the sensor is shown in Section II. The modeling of hysteresis caused by the sensor textile is further described in Section IV to improve the accuracy of the sensor system. Finally, we conducted an experiment for classifying sitting postures to evaluate the quality of the developed sensor system and the modeling (see Section V).

A. Related Work

Pressure sensing on the human body covers a wide field in wearable computing. The activity of different muscles has been measured with force-sensitive foil sensors [10], [11]. Upper arm positions have also been recorded with resistance changing foams [12], [13].

Commercially available nontextile sensor mats have been used to detect the sitting posture in a chair [14]–[16]. One sensing mat covers the back and one the seat surface. These provide a resolution of 1 cm $\times$ 1 cm with 42 $\times$ 48 sensing elements each. A total of 127 pressure distribution maps are recorded each second. With this system, real-time posture detection is possible with a recognition rate of 96% in average. In [17], the sensor amount has been reduced to 19 discrete force-sensitive foil sensors that reach a classification accuracy of still 78%.

Measuring sitting postures can serve as measure for healthy sitting behavior or as user interface [14], [15]. They can also be used to identify a driver in a car [18], evaluating his behavior [19], or as measure for comfort [20] or physical wellness [21].

II. Sensor Design

The developed pressure measurement system consists of two separate parts (see Fig. 1): the textile sensor array and the measurement electronics. Electrical signals were routed by textile wires on the sensor textile and connected to the measurement and communication electronics.

A. Architecture of the Textile Sensor

The textile sensor consists of a basic three-layer structure, forming a variable capacitor. Between two electrodes made of conductive textile, a compressible spacer is arranged that varies its thickness dependent on the pressure induced. Additional

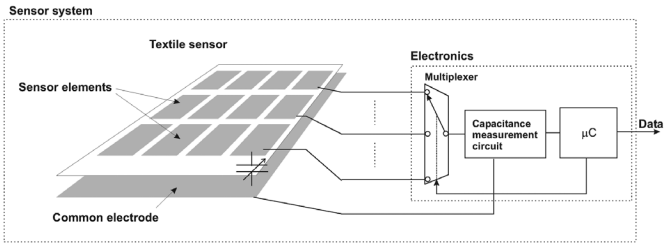

Fig. 1. Overview of the sensor system. The sensor elements are individually connected to the measurement unit.

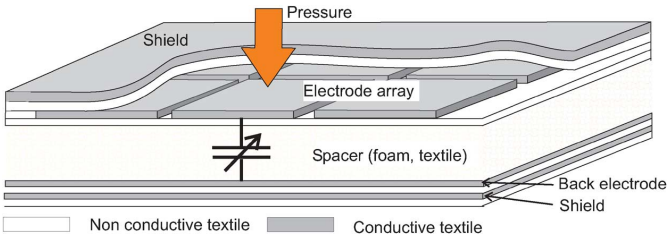

Fig. 2. Array of electrodes of conductive yarn on one side and a common electrode on the other side of the spacer form the capacitors for pressure sensing.

layers of conductive textile are arranged covering both sides of the array for shielding purposes.

The capacitance C of a parallel-plate capacitor of area A is inverse proportional to the distance d between the plates (electrodes) at a given permittivity ϵ of the material between the plates, i.e.,

$$C = \epsilon \frac{A}{d}. \tag{1}$$

1) Electrodes: Single electrodes are arranged on one side of the spacer as an array, while the other side consists of one common electrode (see Fig. 2), forming the capacitors between each electrode and the common electrode. The single electrodes are embroidered with conductive yarn. The common electrode consists of a silver-coated woven textile.

The needed pressure sensitivity of the sensor is defined by the application: pressure induced by sitting has been measured as up to 3 $\mathrm{N/cm^2}$ in the region of the pelvic bone. For muscle activity, it varies from 0 to around 1 $\mathrm{N/cm^2}$, and up to 0.7 $\mathrm{N/cm^2}$ for compression stockings in the highest class IV [22].

The size of the electrodes is 2 cm $\times$ 2 cm for both types of sensors. The electrodes of the sensor arrays have a spacing of 0.7 mm. This grid distance of 2.7 mm is defined by the embroidering process: the needles of the embroidering machines are 2.7 mm in distance. Measurements of the pressure distribution with a commercial available system from *Tekscan* with 1 cm $\times$ 1 cm resolution have shown that the smallest part of the buttock, back, legs, and upper arms (bone at the buttock) can be recognized with a resolution of 3 cm $\times$ 3 cm.

2) Connections to the Electrodes: Each electrode of the sensor has to be connected separately. Connection lines of conductive yarn are embroidered with a spacing of 5.4 mm onto the carrying, nonconductive textile to its border where the electronics is connected. The connection from the connection lines to the electronics is implemented by tying the conductive yarn together with copper wires in the prototype.

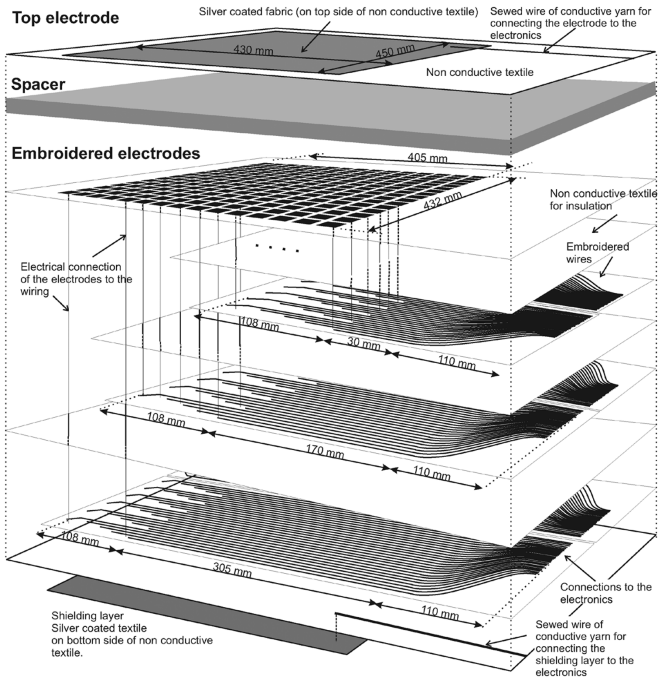

Fig. 3. Construction of the textile sensor with 240 sensor elements. Due to the amount of sensors, three layers are needed for the embroidered connections to the electrodes.

Due to the amount of sensors, three layers are needed for routing the connections of the sensor with 240 sensing elements. These layers are separated by layers of nonconductive, woven textile to insulate the lines from the electrodes below. Any kind of close meshed textile can be used for this purpose. The connection layers are manufactured in three different lengths and for half the width of the array. Each connects 5 $\times$ 8 electrodes, mirrored in the middle of the array (see Fig. 3). Connection of the measuring lines to the electrodes is achieved by sewing the lines over the electrodes through the separating layers. The longest connection lines are arranged at the outer side, so that no connection lines of other layers are crossed by sewing.

3) Conductive Yarn: The resistance of the sewed connections plus the resistance of the lines has to be below 5 $\mathrm{k\Omega}$ due to the used measurement principle. The yarn has to be uncoated at the points of connection, and must have a sufficient connecting surface, e.g., the conductive part of the yarn has to be at the outside and not enclosed by the carrier.

The yarn used, for all conductive, embroidered parts, is a multifilament yarn coated with silver. It is available from *Statex*, type Shieldex 235/34dtex 2ply HC. It has a resistance of 120 $\mathrm{\Omega/m}$ that increases only a few percent after washing ten times.

4) Spacer: The spacer between the electrodes defines the pressure range and the resolution of the sensor. A replaceable spacer enhances the flexibility of the sensor system since the spacer can be chosen according to the desired range and resolution. When selecting the spacer, the focus can be set to criteria such as pressure range, comfort (textile feeling, breathable), and robustness, instead of having good linearity due to the modeling.

For measuring sitting pressure patterns, a textile spacer manufactured by Müller Textil, Germany, has been chosen. It is a

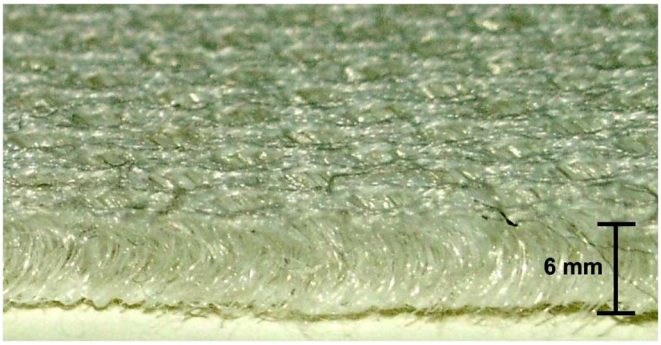

Fig. 4. Textile spacer (Müller Textil, Germany) with 6 mm thickness and compressibility of 50% at 2.3 $\mathrm{N/cm^2}$.

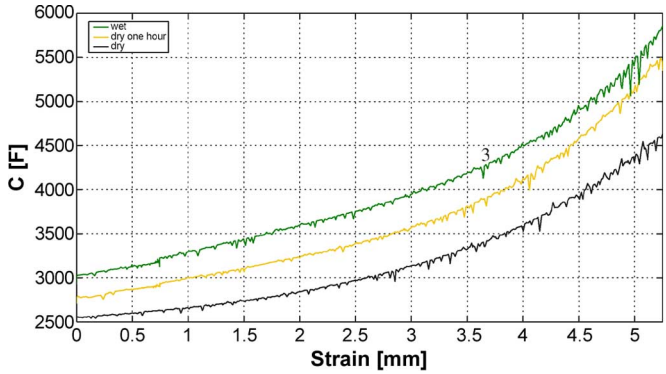

Fig. 5. Capacitance of a wet sensor compared to dry condition and after 1 h of drying.

3-D knit fabric that consists of polyester pile yarns that connect both sides of the spacer, forming a kind of spring (see Fig. 4). The pile yarns are bent while compression is applied what results in a counteracting force. We used the product with 6 mm thickness and compressibility of 50% at 2.3 $\mathrm{N/cm^2}$. Pressure induced by sitting has been measured as up to 3 $\mathrm{N/cm^2}$ in the region of the pelvic bone. The used spacer fits well in this pressure range, is comfortable to sit on, breathable, and robust.

B. Measurement Electronics

The measured capacitance of a single electrode of the prototype varies from 3.2 pF uncompressed to 5.5 pF at a pressure of 12 $\mathrm{N/cm^2}$. The electrodes in the sensor array are measured sequentially, each after the other, switched by a multiplexer (electronic switch) (see Fig. 1). The electrodes not connected to the measurement circuit and the shielding layers on both sides of the sensor are connected to ground so that the active one is surrounded by a ground-shield to connect parasitic capacitances to ground.

The parasitic capacitances are in the range of 100 pF for the active electrode to ground and about 150 pF for the common electrode to ground. To reduce the effect of these parasitic capacitances, the two-port measurement method is applied [23]. With this method, parasitic capacitances are connected to ground, and the capacitance between the electrodes is measured separately from the ground potential.

The capacitance to digital converter AD7745 from Analog Devices is used to measure the capacitance of the sensor elements. It is a sigma--delta converter that measures the capacitance in a range of ± 4 pF with an adjustable offset between 0 and 17 pF and an accuracy of 4 fF at a rate of 90 Hz. A microcontroller drives the AD7745 and multiplexer, and sends the data via universal serial bus (USB) to a PC.

III. Permittivity of the Spacer

The compressible spacer between the sensor electrodes has an impact on the capacitance measurement by its permittivity. The influence by the variation of the permittivity due to compression is eliminated by calibrating the sensor. Changes of permittivity over time, not induced by pressure changes, influences the measurement. Such alternations could occur due to aging and changes in the material of the spacer, humidity, or temperature.

A. Temperature Dependence

Permittivity of the textile spacer has been measured for temperatures between 10 °C and 30 °C. No significant change has been detected. It was below the accuracy of the measurement of 4 fF.

B. Humidity Dependence

The permittivity of the textile spacer has been measured for a humid spacer (95% relative humidity) and no difference has been recorded compared to the capacitance values at about 60% relative humidity. The textile spacer mainly consist of air in the uncompressed state; the volume fraction of material is less than 5%. Relative permittivity ϵ_r of dry air is about 1.0006 and that of water is 80. For a relative humidity of about 60% at 20 °C, the water vapor in the air is about 10 $\mathrm{g/m^3}$ or 10 ppm. This results to a relative permittivity of humid air at 60% of about 1.0014.

If there is condensing humidity and the spacer is wet, changes in permittivity become significant since the amount of water is higher than when no condensing occurs. A completely wet spacer increases the permittivity to that of water, meaning factor 80.

The relative permittivity $\epsilon_r(\mathrm{wet})$ for a wet spacer with relative volumetric content V_w of water is expected as

$$\epsilon_r(\mathrm{wet}) = \epsilon_r(\mathrm{dry})(1 - V_w) + \epsilon_r(\mathrm{water})V_w. \qquad (2)$$

If the spacer consists of 0.2% water, $\epsilon_r(\mathrm{wet})$ is expected to be 1.16.

The measured change in capacitance between a dry and a wet sensor can be seen in Fig. 5. The increase of the permittivity is not constant over the whole compression range since the amount of water also changes due to different fluctuations of air and water out of the sensor. The amount of water in the sensor was 0.2% in wet state. The measured change in capacitance between wet and dry spacers is 1.19 at zero compression and 1.25 when the spacer is compressed to 30% thickness. After 1 h of drying at normal room conditions, a reduction in the measured capacitance toward the dry condition can be recorded.

The sensor has to be protected from getting wet, e.g., by enclosing with waterproof textiles like Goretex.

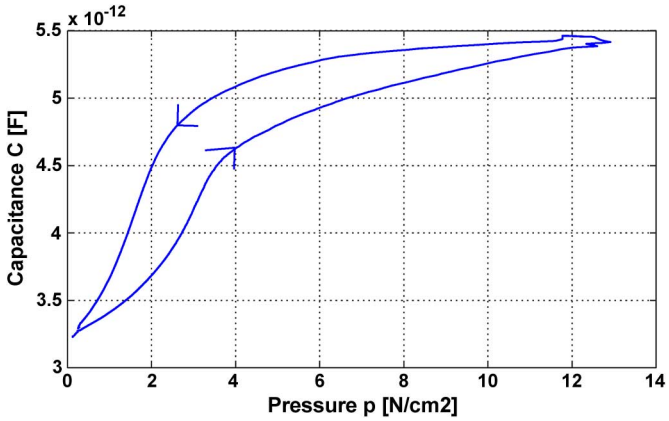

Fig. 6. Hysteresis in the pressure--capacitance diagram of a single sensing element with the textile spacer of 6 mm thickness.

IV. Hysteresis Modeling

The compressible spacer between the electrodes provokes hysteresis (see Fig. 6). The hysteresis leads to a maximal difference greater than 50% of measured pressure between the upper and lower branches of the hysteresis curve when a cycle is performed from 0 to 10 $\mathrm{N/cm^2}$ and backward. If the pressure is just calculated from the mean of the maximal and minimal reachable pressure values at a given capacitance, the resulting error is in the range of up to 20%--30%.

The hysteresis curve is not constant over time, like in a magnetic material. The distance of the upper and lower bounds of the hysteretic curve also depend on the time and pressure induced. A shift toward higher compression can be observed under load.

Hysteresis is caused by friction in the spacer material. Friction occurs between the polyester pile yarns of the textile spacer or in the cell walls of foams and the inner molecular structure. This force is directed in the opposite direction of the movement that causes the hysteresis. The dissipated energy within one cycle corresponds to the area enclosed by the hysteresis curve in the force–strain diagram.

To reduce the influence of the hysteresis on the measurement result, the behavior of the spacer has been modeled. With this approach materials with different hysteresis behavior can be used what enhances the flexibility in spacer selection.

A. Preisach Model

Models to describe hysteresis are mentioned in [24]. In this paper, we used the Preisach model [25]. This model is known in the area of magnetics [26], [27] to describe the hysteretic behavior of magnetic material. With the Preisach model, a simple calibration of the sensor is possible since its parameters are defined with a reference measurement. The model has a low computation complexity, so that it can be integrated, e.g., onto a microcontroller for online pressure calculation. The model can be implemented for any continuous, closed-loop hysteresis curve.

The Preisach model is based on a superposition of an infinite amount of relay operators $\gamma_{\alpha\beta}$ which values are either -1 or 1. The variables α and β are switching numbers where the value of the operator changes by raising or falling input $u(t)$, respectively

$$\gamma_{\alpha\beta}(t) = \begin{cases} -1, & \text{if } (t) \le \beta \\ \gamma_{\alpha\beta}(\max t_M), & \text{if } \beta < u(t) < \alpha \\ 1, & \text{otherwise} \end{cases} \tag{3}$$

with $t_M := \tau \in [0,t] | (u(t) \ge \beta \cup u(t) \le \alpha)$.

These operators are multiplied with the weight function $\mu(\alpha,\beta)$. The output hysteresis is defined as

$$h(t) = \iint_{\alpha \ge \beta} \mu(\alpha,\beta)\gamma_{\alpha\beta}u(t)d\alpha d\beta \tag{4}$$

with $u(t)$ being the input, the measured capacitance, or the compression of the spacer in our sensor.

For hysteresis with closed major loops, the function $\mu(\alpha,\beta)$ is restricted to a triangle T on the α,β plane [28]. Outside this triangle, $\mu(\alpha,\beta)$ is equal to zero. The interface between points where $\gamma_{\alpha\beta} = 1$ and $\gamma_{\alpha\beta} = -1$ is a stair line with edge points where the input $u(t)$ has local maxima M and minima m. The model can be approximated by setting up an equidistant grid over T and discretize t [29]. The integral is transformed into a sum. $h\ (t)$ can be rewritten as

$$h(t) = x(t) - 2F\left(M_{n(t)}, u(t)\right) \tag{5}$$

$$x(t) = 2\sum_{k=1}^{n(t)-1}\left[F(M_k, m_{k-1}) - F(M_k, m_k)\right] + 2F\left(M_{n(t)}, m_{n(t)-1}\right) - F(\alpha_0, \beta_0) \tag{6}$$

for falling input, and

$$h(t) = x(t) - 2F\left(u(t), m_{n(t)-1}\right) \tag{7}$$

$$x(t) = 2\sum_{k=1}^{n(t)-1}\left[F(M_k, m_{k-1}) - F(M_k, m_k)\right] - F(\alpha_0, \beta_0) \tag{8}$$

for raising input.

$x(t)$ is constant until a local maximum M or minimum m of the input $u(t)$ is generated or deleted. If an extremum in the input is generated, $x(t)$ is given by

$$x(t) = h\left(t_{M_l}\right) : t_{M_l} < t \tag{9}$$

for falling input and

$$x(t) = h\left(t_{m_l}\right) : t_{m_l} < t \tag{10}$$

for raising input.

Each local minimum m_k of the input is removed from the history if it is larger than the input $u(t)$ when the input is falling. When input rises, all local maxima M_k that are smaller than the actual input were deleted.

The weight function $\mu(\alpha,\beta)$ can be calculated for a point (α,β) in the triangle T as [30]

$$\mu(\alpha,\beta) = -\frac{1}{2}\frac{\delta^2 F(\alpha,\beta)}{\delta\alpha\delta\beta} \tag{11}$$

$$F(\alpha,\beta) = \frac{1}{2}(h_\alpha - h_{\alpha,\beta}) \tag{12}$$

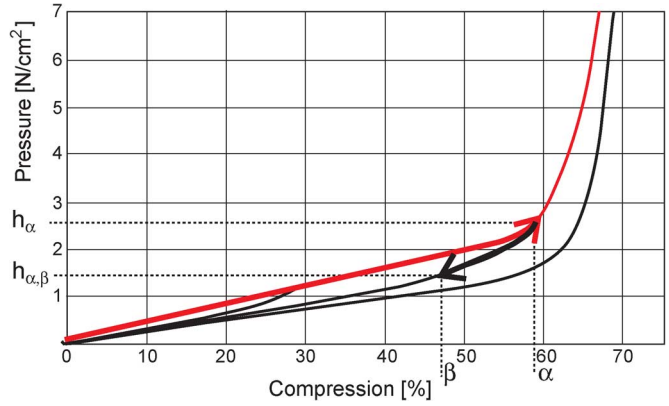

Fig. 7. Parameter definition of the model. h_α is defined by a rising bounding curve and $h_{\alpha,\beta}$ by falling curves.

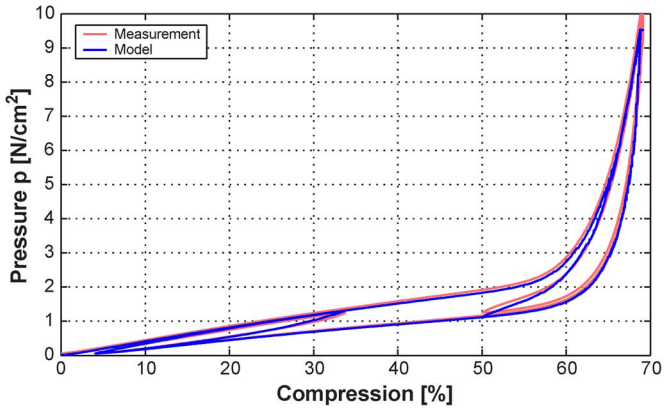

Fig. 8. Pressure p from the output of the model compared to the measured pressure dependent on the compression.

where h_α represents the desired output $h(t)$ when $u(t)$ increases from negative saturation to $u(t) = \alpha$. If $u(t)$ decreases afterward to value β, the output is $h_{\alpha,\beta}$.

Calculating $h(t)$ for one time step is reduced to one addition of previous calculated $x(t)$ with the corresponding value of the matrix F when no extremum in the input $u(t)$ is generated. Otherwise, a sum over the values of F corresponding to all previous extremum has to be evaluated. $2n+2$ summations and two multiplications have to be performed in this case (with n the number of extrema).

B. Identification of Parameter Values

The values of the model parameters are defined with measuring pressure, depending on the compression of the spacer or the measured capacitance. The model parameters $F(\alpha, \beta)$ are calculated according to (12) by increasing the input (compression or alternatively capacitance) to the value $\alpha \in [0, \alpha_{\max}]$. h_α is set to the pressure at this point. Then the input is decreased to the value $\beta \in [0, \alpha]$ and $h_{\alpha,\beta}$ set to the pressure at the new point (see Fig. 7). To define the full F matrix, points have to be evaluated for each combination of α and β. The value $\alpha_{\max}$ is chosen so that the whole desired pressure range is covered.

To define the values of h_α for the textile spacer, the pressure has been increased from $h_0 = 0\,\mathrm{N/cm^2}$ to $h_{\alpha\max} = 10\,\mathrm{N/cm^2}$. To define $h_{\alpha,\beta}$, practice has shown that the model is accurate enough, if only three falling curves for three different α are measured and the remainder are interpolated. Curves falling from 10, 2.3, and 1.2 $\mathrm{N/cm^2}$ have been recorded (see Fig. 7). These points have been chosen depending on the shape of the curve. In the region of 2.5 $\mathrm{N/cm^2}$, the derivative of the pressure with respect to compression is changing, as can be seen in Fig. 7. The starting points of these curves have to be adopted according to the spacer used.

With the used tensile test machine (Zwick/Roell DO-FB0. 5TS), the parameters of the model can be evaluated within less than 2 min of measurement by measuring force and strain of the compressed spacer.

C. Results

The model has been evaluated by modeling the hysteresis of the textile spacer. The pressure runs through a cycle from 0 to 10, 1.3, 10, 0, 1.3, and back to 0 $\mathrm{N/cm^2}$ (see Fig. 8). This cycle has been repeated 50 times continuously during 2 h with four different samples of the spacer. On the one hand, the pressure has been measured by the test machine, and on the other, modeled with the Preisach model by using the strain as model input.

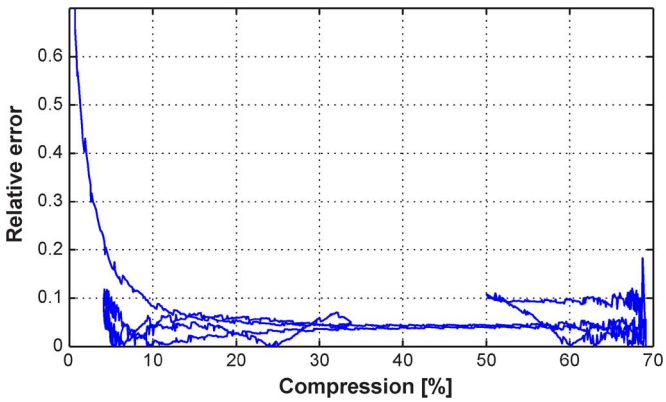

Fig. 9. Relative error of model output compared to the measured pressure dependent on the compression for three different cycles (same cycles as shown in Fig. 8).

Fig. 10. Textile sensor with 240 elements (same as shown in Fig. 3) used for sitting posture measurement. 1: common electrode, 2: spacer, 3: sensing electrodes, and 4: electrodes switched to ground.

The modeled and measured pressure curve for one cycle can be seen in Fig. 8 and the corresponding error curve in Fig. 9. By using the Preisach model, the maximal error induced by hysteresis of the textile spacer could be reduced from 50%

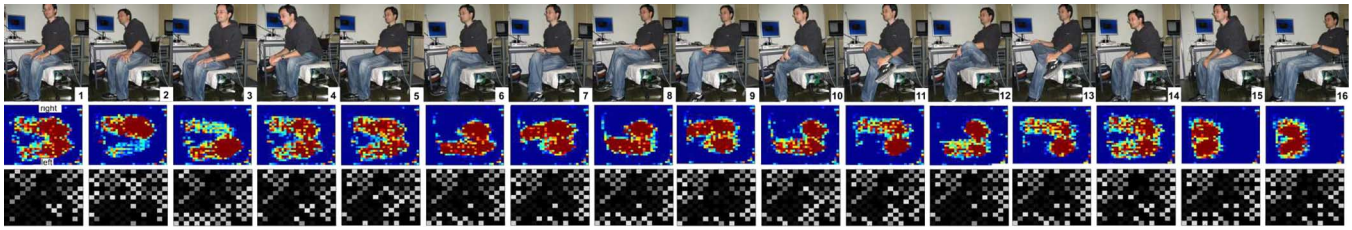

Fig. 11. (Top) Sixteen different sitting postures have been performed and the pressure patterns measured with the reference sensor (middle) and the textile pressure sensor (bottom) (for numbers see text).

below 10% between modeled and measured pressure curve in the range of 0.5–3.5 $\mathrm{N/cm^2}$. For higher pressure, the maximal error increased up to 34% over all cycles. The average error was reduced from 24% to around 5% up to 3.5 $\mathrm{N/cm^2}$ and 8% for 3.5 $\mathrm{N/cm^2}$ to 10 $\mathrm{N/cm^2}$.

V. Classification of Sitting Postures

To evaluate the developed textile pressure sensing system, we conducted a study in which recorded pressure patterns were used for the classification of 16 sitting postures. The influence on the classification accuracy by compensating the hysteresis has been measured with an experiment.

A. Experiment Setup

A total of 96 out of 240 sensor elements of the pressure mat have been preselected, forming a checkerboard pattern, to investigate the robustness of the sensor system and increase the speed for measuring a whole pattern. The sensing elements cover an area of 35.1 cm × 40.5 cm. The textile spacer with 6 mm thickness has been used, resulting in an overall thickness of the mat of 1.1 cm (see Fig. 10).

A commercially available pressure mat from *Tekscan*[1] has been placed below the textile sensor for reference. This mat measures the pressure on the seat with 1024 sensor elements 20 times a second at a relative accuracy of 10%. The *Tekscan* sensor is a flexible plastic mat with discrete pressure sensors mounted. The mat has been calibrated before use with the calibration system from *Tekscan* in the range of 0–3.3 $\mathrm{N/cm^2}$. Placing the reference sensor below the textile mat does not influence the pressure distribution over the textile sensor. The two sensor systems have been synchronized so that only the frames of the reference systems are used with a timely corresponding frame of the textile sensor system.

Both sensor systems have been mounted on a chair with a flat surface. The height of the chair has been adapted to the length of the legs of the subjects, so that, while sitting upright, their heels are touching the floor and their legs the front of the seat.

The pressure on the back of the chair has been measured with a textile sensor with a single sensing element separately. No reference sensor has been placed there.

B. Experiments

The following 16 postures have been measured for each subject (see Fig. 11): seated upright (1), leaning right (2), left (3), forward (4), back (5), left leg crossed over the right (6), right over left (7), once seated upright and once leaning back (8) and (9), once while the knees are touching and once with the ankle rested on the leg (10)–(13), slouching (14), sitting on the leading edge (15), and slouched down (16). For postures without leaning back, the back of the chair is not touched. Each posture has been held for 30 s. A home position (sitting upright) has been adopted for 5 s between each succeeding position to define the transitions between the postures. Examples of patterns measured by the *Tekscan* system and the textile sensor can be seen in Fig. 11.

The back sensor is giving a signal of a pressure of 0.06 $\mathrm{N/cm^2}$ with a standard deviation of 0.07 $\mathrm{N/cm^2}$ for the postures without leaning back and 1.8 $\mathrm{N/cm^2}$ with a standard deviation of 0.34 $\mathrm{N/cm^2}$ for leaning back.

The experiment has been conducted with nine subjects (six males and three females) in three rounds. In each round, each position beside the home position has been taken once.

C. Classifier and Features

Naive Bayes classifier [31] has been used as learning algorithm. The following features have been tested for classification:

1) sensor value from each sensor element;
2) center of force;
3) pressure applied to 4 and 16 equal aggregated areas of the seating area.

A reduced set of k features that reaches best classification accuracy has been searched with the sequential forward selection (sfs) algorithm [32] (k-best features). As cost function, J the mean of the classification accuracy of the cross validation over all subjects (leave-one-person-out) has been used. The number k of features is chosen so that the highest classification accuracy has been reached.

The following 16 best features have been found by sfs algorithm (see Fig. 12):

1) values of sensor elements number 9, 10, 16, 31, 34, 38, 39, 56, 62, 65, 86, 89, 91, 96, and the back sensor;
2) x-coordinate of center of force (sideward);
3) one of the 16 equal aggregated areas (no. a7).

The sensor values have been preprocessed before calculating the features; when certain sensor elements were failing, which can occur spontaneously, their data have been interpolated by the mean of the adjacent elements.

D. Classification Results

To determine the effect of the hysteresis on the classification result, classification was carried out once with the data from the textile sensor and once with the data where the hysteresis with the Preisach model introduced in Section IV-A has been compensated, both with leave-one-person-out cross validation.

[1]Tekscan ConfortMat from Tekscan, Inc., South Boston, MA.

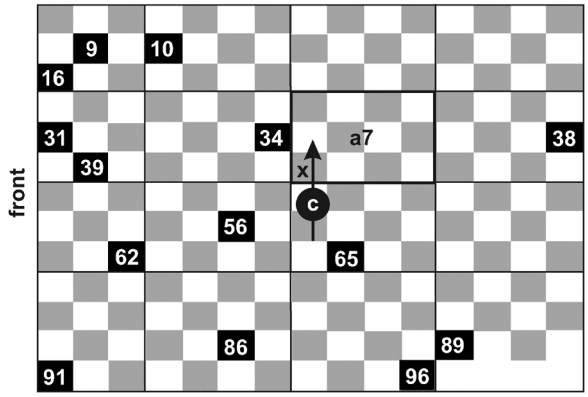

Fig. 12. 16 best features selected by sfs algorithm (black: selected sensor elements, c: center of force, a7: selected area, gray: connected sensor elements).

TABLE I
RECOGNITION RATE FOR DATA FROM THE TEXTILE SENSORS AND THE REFERENCE SYSTEM

Data	only seat sensor	with back sensor
Without hysteresis compensation	55%	81%
Hysteresis compensated	59%	82%
Reference system	56%	84%

Without hysteresis compensation, the recognition rate is 55% without and 81% with the back sensor. The average recognition rate for the data with compensated hysteresis increases to 59% without and 82% with the back sensor (see Table I). The rate is improved by 6.8% and 1.2% compared to using the data containing hysteresis.

The classification accuracy reached with the data of the *Tekscan* mat recorded simultaneously is 56% without back sensor with features optimized for the *Tekscan* data. If the data of the textile back sensor is added, the recognition rate is increased to 84%.

VI. CONCLUSION

A pure textile pressure sensor has been designed and evaluated to measure pressure distribution on the human body. This opens the field for long-term operation for medical applications such as supervision of sitting postures, decubitus prevention, muscle activity measurements [33], or control of pressure in medical stockings.

The Preisach model has been implemented to quantify hysteresis of the sensor. Only with this modeling, it is possible to achieve accurate pressure values from the textile sensor with material that has not been optimized for this application. The average error of measured pressure could be reduced from 24% to below 5% for cyclic pressure change up to a duration of 2 h. The spacer used does not have to be optimized for linearity and low hysteresis. The models can be easily adopted for other designs or types of pressure sensors and strain sensors, and only the model parameters have to be reevaluated. The influence of tolerances by manufacturing on the measured pressure can be reduced with the model by recalibrating each sensor separately.

The textile pressure sensor has been used for classification of sitting postures with comparable classification accuracy as in the related work [17]. The textile sensor performs similarly to the commercial system for this application. Compensating hysteresis by modeling the sensor behavior increases the classification results between 1% and 7%, even though the error of measured pressure is reduced by factor 5 with the hysteresis modeling. The main benefit of the hysteresis modeling can be recognized more in applications where exact pressure values are needed, e.g., decubitus prevention, muscle activity measurements, or control of pressure in medical stockings, but is not as significant for posture classification.

ACKNOWLEDGMENT

The authors would like to thank B. Bischoff and R. Ferrario from Bischoff Textil AG, St. Gallen, Switzerland, for their support in manufacturing the sensor textile.

REFERENCES

[1] D. Roggen, B. Arnrich, and G. Tröster, "Life style management using wearable computer," presented at the 4th Int. Workshop Ubiquitous Comput. Pervasive Healthcare Appl., UbiHealth 2006, Newport Beach, CA, Sep. 2006.

[2] M. Stäger, H. Junker, M. von Waldkirch, and G. Tröster, "Using wearables in maintenance: A modular test platform," presented at the Workshop Wearable Computing (TCMC 2003), Graz, Austria, Mar. 2003.

[3] I. Maurtua, P. T. Kirisci, T. Stiefmeier, M. L. Sbodio, and H. Witt, "A wearable computing prototype for supporting training activities in automotive production," in *Proc. 4th Int. Forum Appl. Wearable Comput. (IFAWC)*, Mar. 2007, pp. 45–56.

[4] T. Stiefmeier, D. Roggen, G. Troster, G. Ogris, and P. Lukowicz, "Wearable activity tracking in car manufacturing," *IEEE Pervasive Comput.*, vol. 7, no. 2, pp. 42–50, Apr.–Jun. 2008.

[5] M. Klann, "Playing with fire: Participatory design of wearable computing for fire fighters," in *Proc. Conf. Hum. Factors Comput. Syst.*, Apr. 28–May 3 2007, pp. 1665–1668.

[6] M. Sergio, N. Manaresi, F. Campi, R. Canegallo, M. Tartagni, and R. Guerrieri, "A dynamically reconfigurable monolithic CMOS pressure sensor for smart fabric," *IEEE J. Solid-State Circuits*, vol. 38, no. 6, pp. 966–975, Jun. 2003.

[7] C. Mattmann, T. Kirstein, and G. Tröster, "A method to measure elongations of clothing," presented at the 1st Int. Sci. Conf. Ambience, Tampere, Finland, Sep. 2005.

[8] I. Locher, T. Kirstein, and G. Tröster, "Temperature profile estimation with smart textiles," presented at the Int. Sci. Conf. Ambience, Tampere, Finland, Sep. 2005.

[9] I. Locher, M. Klemm, T. Kirstein, and G. Tröster, "Design and characterization of purely textile patch antennas," *IEEE Trans. Adv. Packag.*, vol. 29, no. 4, pp. 777–788, Nov. 2006.

[10] P. Lukowicz, F. Hanser, C. Szubski, and W. Schobersberger, "Detecting and interpreting muscle activity with wearable force sensors," in *Pervasive (Lecture Notes in Computer Science)*, ser. , K. P. Fishkin, B. Schiele, P. Nixon, and A. J. Quigley, Eds. New York: Springer-Verlag, 2006, vol. 3968, pp. 101–116.

[11] O. Amft, H. Junker, P. Lukowicz, G. Tröster, and C. Schuster, "Sensing muscle activities with body-worn sensors," in *Proc. Int. Workshop Wearable Implantable Body Sens. Netw. (BSN 2006)*, Apr. 2006, pp. 138–141.

[12] L. Dunne, R. Tynan, G. O'Hare, B. Smyth, S. Brady, and D. Diamond, "Coarse sensing of upper arm position using body-garment interactions," in *Proc. 2nd Int. Forum Appl. Wearable Comput.*, 2005, pp. 138–141.

[13] L. Dunne, S. Brady, B. Smyth, and D. Diamond, "Initial development and testing of a novel foam-based pressure sensor for wearable sensing," *J. Neuroeng. Rehabil*, vol. 2, no. 4, pp. 2–4, 2005.

[14] L. A. Slivovsky and H. Z. Tan, "A real-time sitting posture tracking system," in *Proc. 9th Int. Symp. Haptic Interfaces Virtual Environ. Teleoperator Syst.*, 2000, vol. 69, pp. 1049–1056.

[15] H. Tan, L. Slivovsky, and A. Pentland, "A sensing chair using pressure distribution sensors," *IEEE/ASME Trans. Mechatronics*, vol. 6, no. 3, pp. 261–268, Sep. 2001.

[16] L. A. Slivovsky, "A real-time sitting posture tracking system," Ph.D. dissertation, Purdue Univ., Washington, DC, 2001.

[17] B. Mutlu, A. Krause, J. Forlizzi, C. Guestrin, and J. Hodgins, "Robust, low-cost, non-intrusive sensing and recognition of seated postures," in *Proc. 20th Annu. ACM Symp. User Int. Softw. Technol. (UIST 2007)*, 2007, pp. 149–158.

[18] A. Riener and A. Ferscha, "Supporting implicit human-to-vehicle interaction: Driver identification from sitting postures," in *presented at the 1st Annu. Int. Symp. Veh. Comput. Syst. (ISVCS 2008)*. Ireland: ACM Digital Library, Jul. 2008, Trinity College, Dublin.
[19] A. Riener and A. Ferscha, "Driver activity recognition from sitting postures," in *Proc. Mensch Comput., Workshop Automotive User Interfaces*, Sep. 2007, pp. 55–63.
[20] M. De Looze, L. Kuijt-Evers, and J. Van Dieen, "Sitting comfort and discomfort and the relationships with objective measures," *Ergonomics*, vol. 46, no. 10, pp. 985–997, Aug. 2003.
[21] M. Prado, J. Reina-Tosina, and L. Roa, "Distributed intelligent architecture for falling detection and physical activity analysis in the elderly," in *Proc. EMBS/BMES Conf.*, 2002, pp. 910–911.
[22] Compression Stockings—Wikipedia, the Free Encyclopedia, 2008. [Online]. Available: http://en.wikipedia.org/wiki/Compression_stockings
[23] F. N. Toth, "Ea design methodology for low-cost, high-performance capacitive sensors," Ph.D. dissertation, Delft Univ. Technol., Delft, The Netherlands, 1997.
[24] P. Sain, M. Sain, and B. Spencer, "Models for hysteresis and application to structural control," in *Proc. Amer. Control Conf.*, Jun. 1997, vol. 1, pp. 16–20.
[25] F. Preisach, "über die magnetische nachwirkung," *Z. für Phys.*, vol. 94, pp. 277–302, 1935.
[26] J. G. Woodward and E. Della Torre, "Particle interaction in magnetic recording tapes," *J. Appl. Phys.*, vol. 31, p. 398, Feb. 1960.
[27] W. J. Fuller Brown, "Failure of the local-field concept for hysteresis calculations," *J. Appl. Phys.*, vol. 33, pp. 1308–1309, Mar. 1962.
[28] I. Mayergoyz and G. Friedman, "Generalized preisach model of hysteresis," *IEEE Trans. Magn.*, vol. MAG-24, no. 1, pp. 212–217, Jan. 1988.
[29] C. Kirchmair, Ein gradientenabstiegsverfahren zum schätzen der parameter des preisach modells für hysterese, 1999, Institut für Informatik, Technische Universität München. München, Germany.
[30] R. B. Gorbet, "Control of Hysteretic Systems With Preisach Representations," Ph.D. dissertation, Univ. Waterloo, Waterloo, ON, Canada, 1997.
[31] R. O. Duda, P. Hart, and D. Stork, *Pattern Classification, 2nd ed*. New York: Wiley, 2000.
[32] J. Kittler, "Feature set search algorithms," *Pattern Recognit. Signal Process.*, pp. 41–60, 1978.
[33] J. Meyer, P. Lukowicz, and G. Tröster, "Textile pressure sensor for muscle activity and motion detection," in *Proc. 10th IEEE Int. Symp. Wearable Comput.*, 2006, pp. 69–72.

Jan Meyer received the Dipl.-Ing. (M.Eng.) degree in electrical engineering in 2003 from the Swiss Federal Institute of Technology (ETH) Zurich, Zurich, Switzerland, where he is currently working towards the Ph.D. degree.

He is currently a Research Assistant in the Wearable Computing Laboratory, Department of Information Technology and Electrical Engineering, ETH Zurich.

Bert Arnrich received Dipl.-Inform. (M.Sc.) degree in natural science informatics and the Dr.-Ing. (Ph.D.) degree from the University of Bielefeld, Bielefeld, Germany, in 2001 and 2006, respectively.

He is currently a Senior Researcher in the Wearable Computing Laboratory, Department of Information Technology and Electrical Engineering, Swiss Federal Institute of Technology Zurich, Zurich, Switzerland. Within national and European research projects, he is engaged in personal health systems. He was involved in medical data mining, machine learning, and statistical modeling in close cooperation with a heart institute. He developed a data mart system in order to discover patterns of heart disease, patient's response to treatment, and real-time risk stratification. Since 2006, his research on pervasive computing technologies is directed toward paving the way for a pervasive, user-centred, and preventive healthcare model.

Johannes Schumm received the Dipl.-Ing. degree in electrical engineering from Rheinisch-Westfaelische Technische Hochschule Aachen University, Aachen, Germany, in 2006.

He is currently a Research Assistant in the Wearable Computing Laboratory, Department of Information Technology and Electrical Engineering, Swiss Federal Institute of Technology Zurich, Zurich, Switzerland. His research interests include reliability of physiological monitoring systems and probabilistic output of classifiers.

Gerhard Tröster (SM'93) received the M.Sc. degree in electrical engineering from the Technical University Karlsruhe, Karlsruhe, Germany, in 1978, and the Ph.D. degree in electrical engineering from the Technical University Darmstadt, Darmstadt, Germany, in 1984.

He was with Telefunken Corporation, Germany, for eight years, where he was responsible for various national and international research projects focused on key components for integrated services digital network and digital mobile phones. Since 1993, he has been a Professor and the Head of the Wearable Computing Laboratory, Swiss Federal Institute of Technology Zurich, Zurich, Switzerland. His research interest includes wearable computing for healthcare and production, smart textiles, sensor networks, and electronic packaging.